

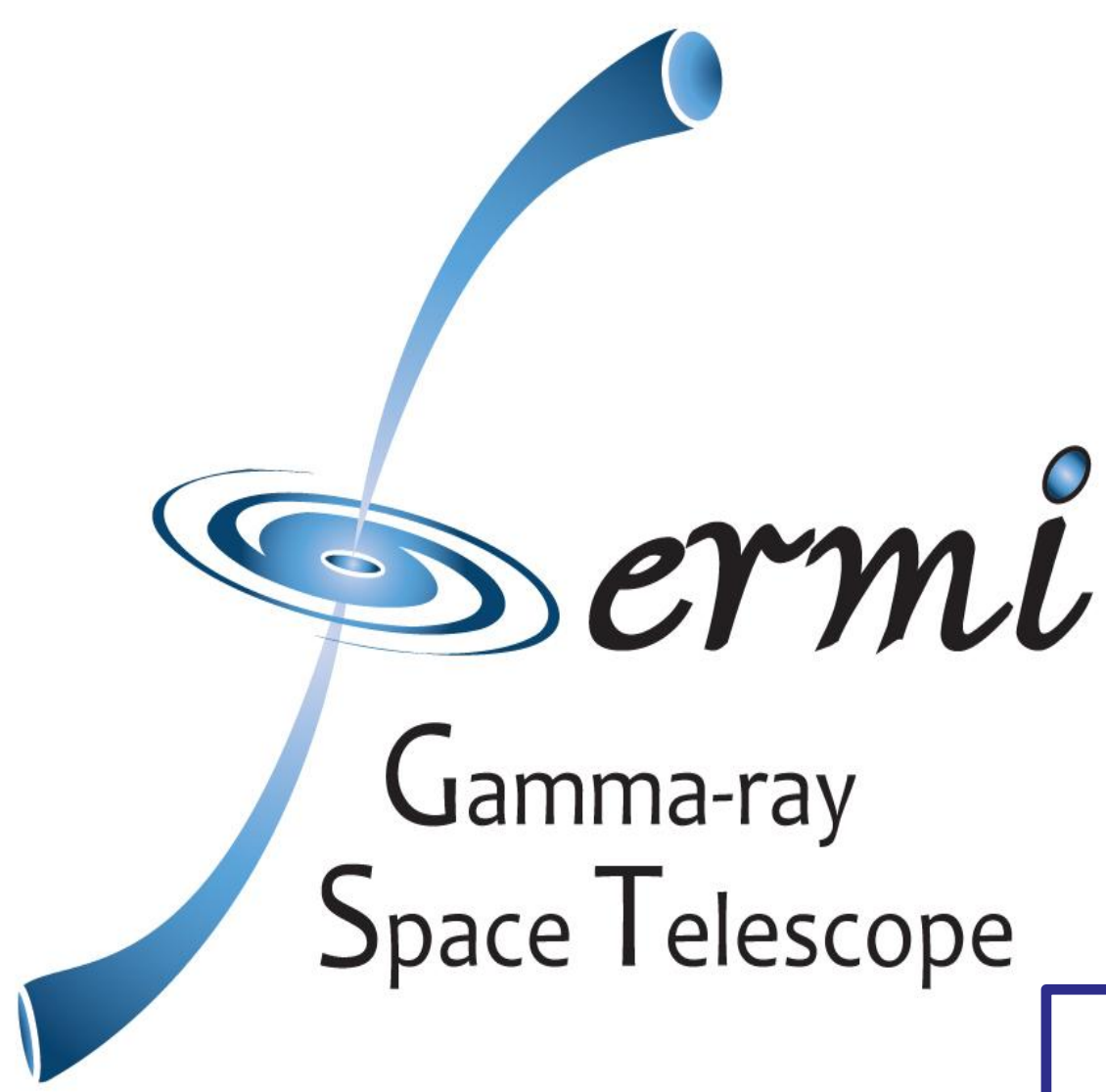
Searches for cosmic ray electron anisotropies with the Fermi-LAT instrument

M. N. Mazziotta¹ and V. Vasileiou²

on behalf of the Fermi Large Area Telescope Collaboration

¹Istituto Nazionale di Fisica Nucleare-Sezione di Bari, via Orabona 4, I-70126 Bari, Italy

²Laboratoire Univers et Particules de Montpellier, place Eugene Bataillon, 34095 Montpellier, France



Abstract

The Fermi Large Area Telescope (LAT) has collected a high statistics sample of high-energy primary cosmic-ray electrons and positrons since the beginning of its operation. The LAT Collaboration has published the first results on the arrival directions of electrons and positrons using the data collected by the Fermi observatory in the first year of operation at energies above 60 GeV. Upper limits on the degree of the anisotropy were set in several energy ranges. We report here preliminary study of the extension of this measurement with 29 months of data and for low energies. The approaches used in this search will be also presented.

1. Introduction

High-energy (>GeV) cosmic ray electrons and positrons (CREs) propagating in the galactic magnetic field lose their energy rapidly through synchrotron radiation and by inverse Compton collisions with low-energy photons of the interstellar radiation field. CREs observed with energies of 100 GeV (1 TeV) originated from relatively nearby locations, less than about 1.6 kpc (0.75 kpc) away. This means that it could be possible that such high energy CREs originate from a highly anisotropic collection of a few nearby sources (possibly pulsars and SNRs). Possible anisotropies in their arrival directions might be associated to the positions of the sources. Alternative scenarios predict anisotropy signals originated by the presence of dark matter (DM) structures within our galaxy.

2. Data analysis and first year results

We have selected a CRE sample consisting of about 1.6×10^6 CRE events with $E > 60$ GeV collected by the Fermi LAT during its first year of operation (M. Ackermann et al. Physical Review D 82 (2010) 092003). The energy threshold has been chosen to minimize the geomagnetic field effects. The starting point of the analysis is the construction of the “no-anisotropy” sky map, that represents the null hypothesis. The search of anisotropies is then performed by comparing the actual sky map with the “no-anisotropy” sky map.

Two techniques have been applied to build the “no-anisotropy” sky map from the original data set:

- **“shuffling technique”**: the arrival times and the reconstructed directions of events in the instrument frame are randomly coupled, generating a set of 100 random sky maps, each one preserving the exposure and the total number of events, and compatible with an isotropic CRE distribution. The final “no-anisotropy” sky map is obtained taking the average of the random maps.
- **“direct integration technique”**: when long term operations are considered, so that any eventual anisotropy is averaged out, it is possible to build a “no-anisotropy” sky map starting from the average rate of events detected as a function of the instrument coordinates (θ, ϕ) and taking into account the pointing history and the exposure.

Two methods have been used to compare the actual sky map with the “no-anisotropy” map:

- **Bin-to-bin comparison**: the comparison between the actual sky map and the “no-anisotropy” one is done by evaluating the significance of each bin. A more powerful search can be done using sky maps with a large number of correlated bins, that are built assigning to each bin the events in a circular region centered on the bin. These maps are sensitive to anisotropies with the same angular scale as the integration radius. No evidences of anisotropies have been found on any energy and angular scale (Figures 1 and 2).

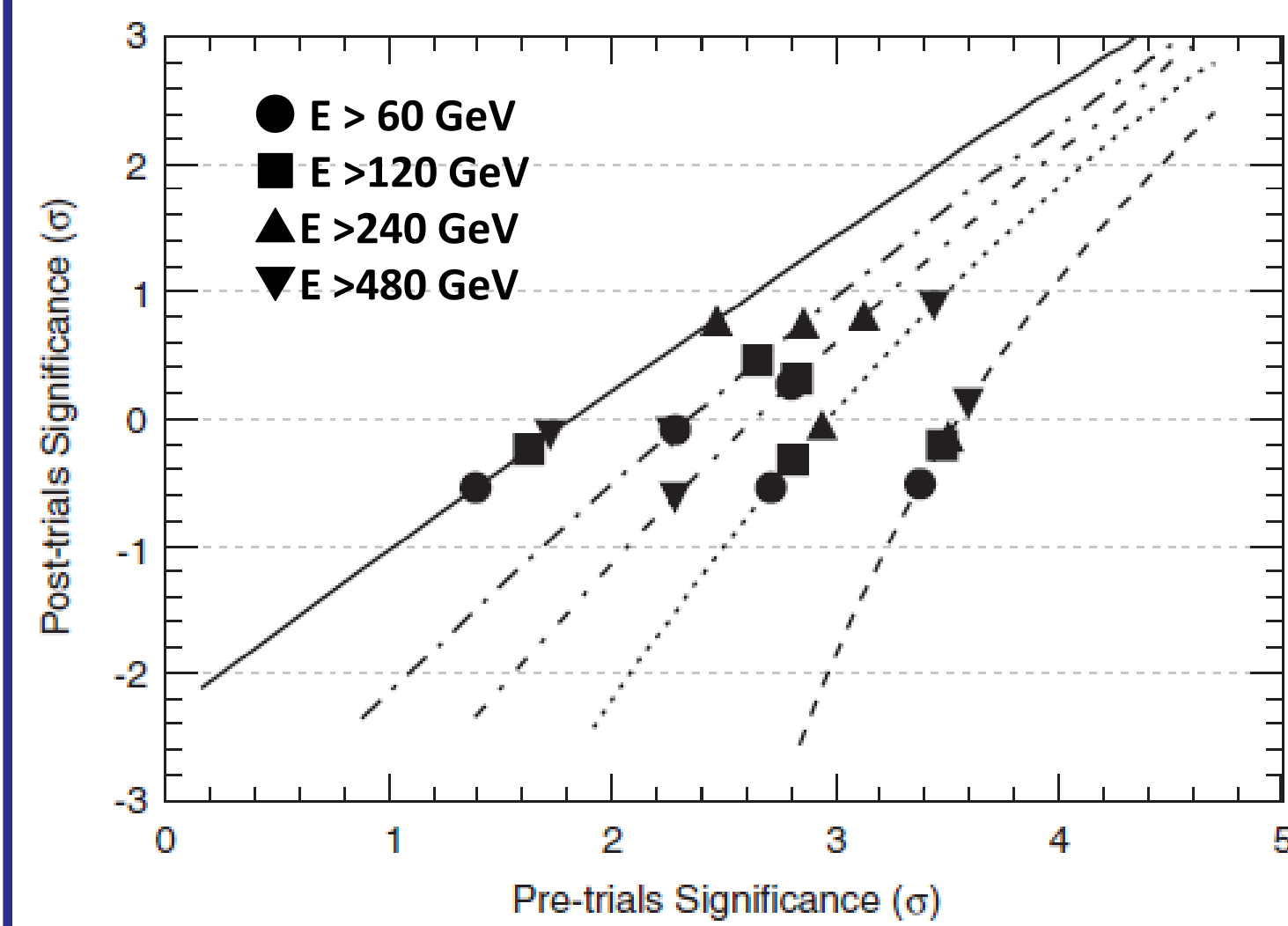


FIG. 1 Curves: correspondence between the pre-trials and significances for integrated maps of different integration radii; from right to left 10, 30, 45, 60, and 90. Points: highest significances in each of the integrated sky maps (one point per minimum energy and integration radius). The highest significance values (points) were all post-trials insignificant.

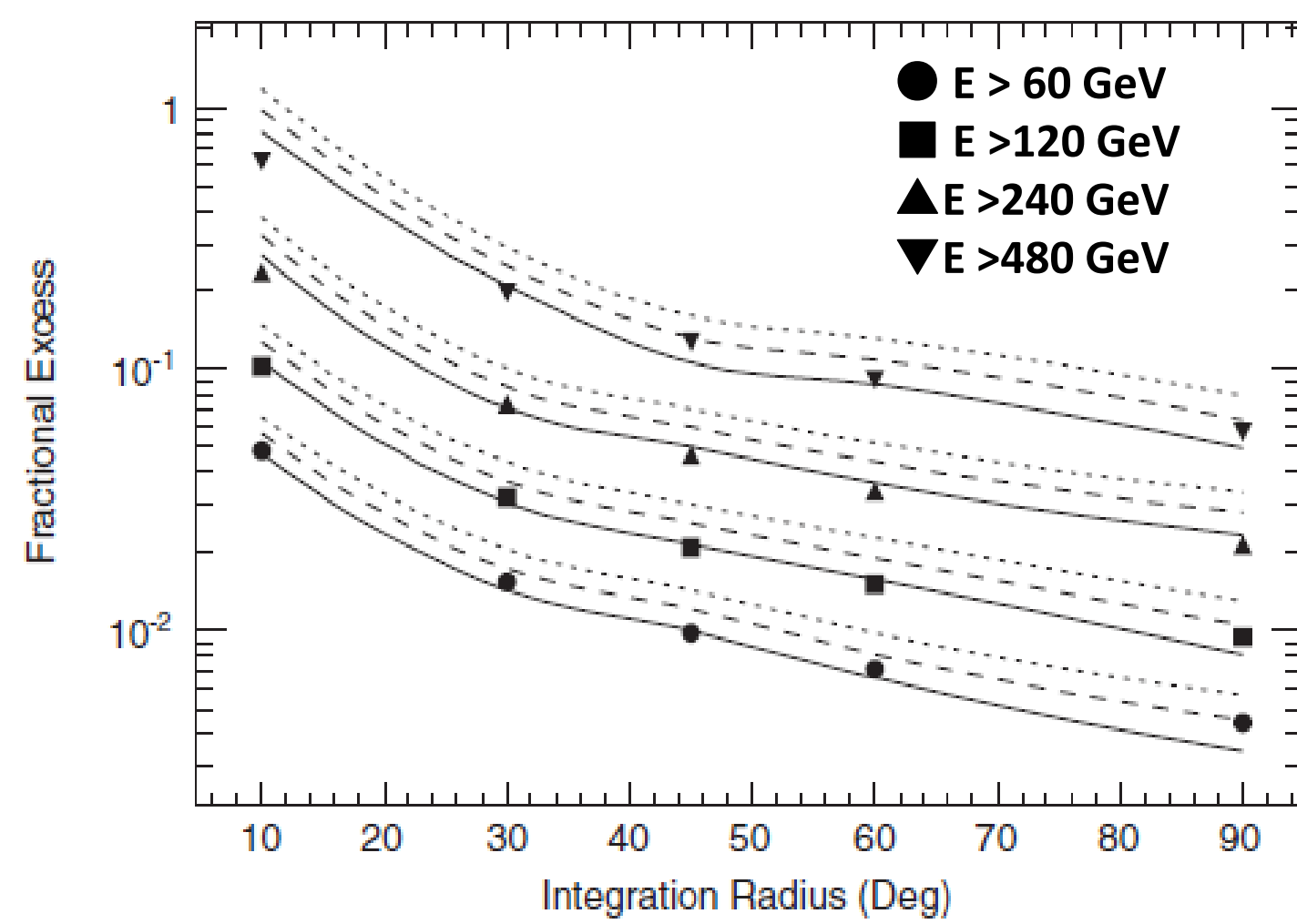


FIG. 2 Points: Fractional excess needed to detect an anisotropy with a post-trials significance versus the integration radius and the minimum energy. Curves: upper limits on the fractional excess. Each group of curves corresponds to a minimum energy. Each line type corresponds to a different confidence level: solid 1σ ; dashed 2σ ; dotted 3σ .

- **Spherical harmonics analysis**: starting from the actual and the “no-anisotropy” sky maps, a fluctuation map is built evaluating in each bin the ratio between the actual events and the “no-anisotropy” events minus one. This map is expanded into spherical harmonics and from the expansion coefficients the angular power spectrum is built. The angular power spectra obtained starting from several energy values are consistent with the absence of anisotropies (Figure 3). This approach allows to set upper limits on the observed anisotropy, and in particular on the degree δ of dipole anisotropy (Figure 4).

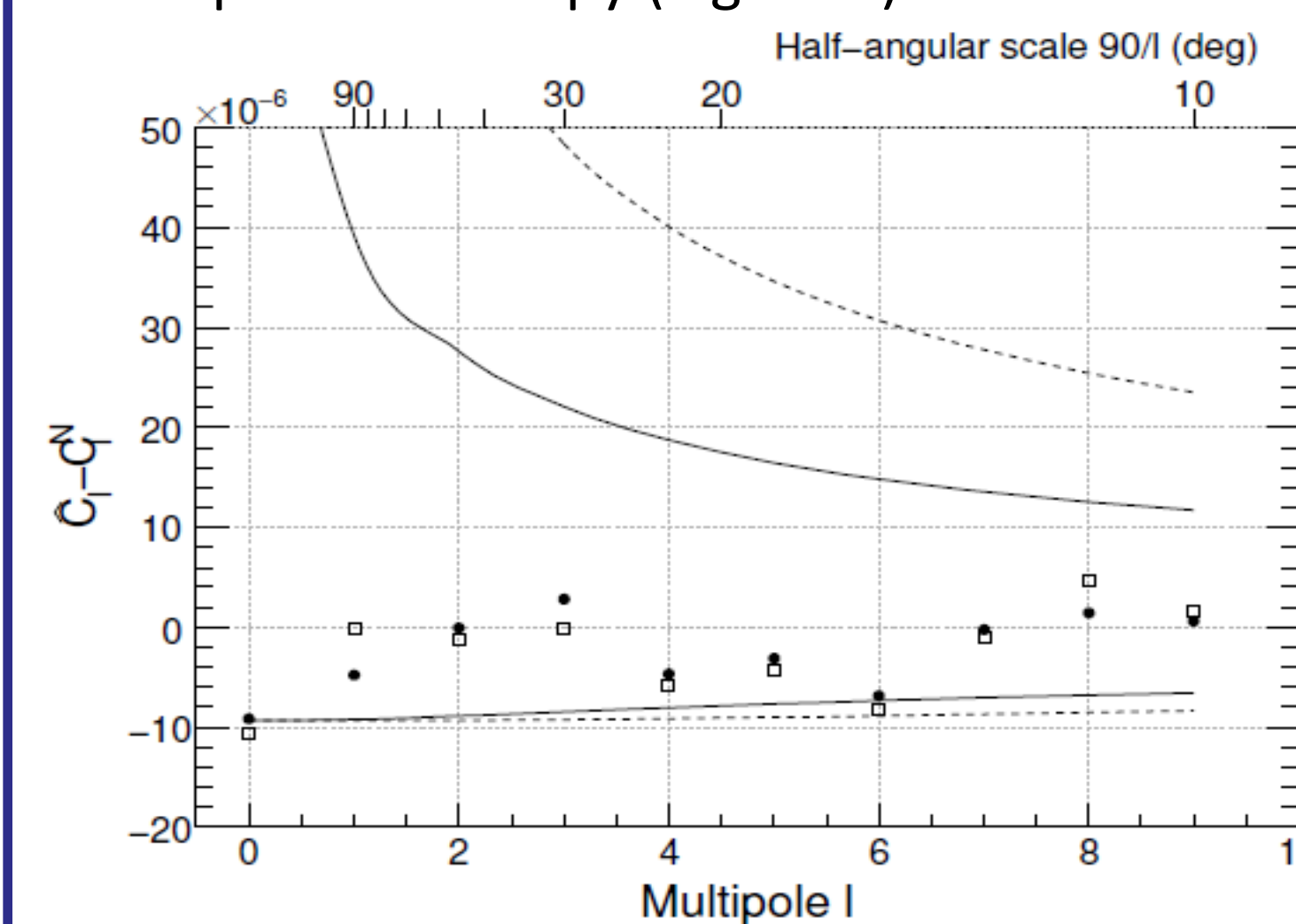


FIG. 3 Angular power spectrum of CREs with a minimum energy of 60 GeV, evaluated with the shuffling technique (full dots) and with the direct integration method (open squares). The solid and dashed lines show respectively the 3σ and 5σ intervals of the probability distribution for the white noise power spectrum. Upper limits on the dipole anisotropy δ as calculated using the C_l values.

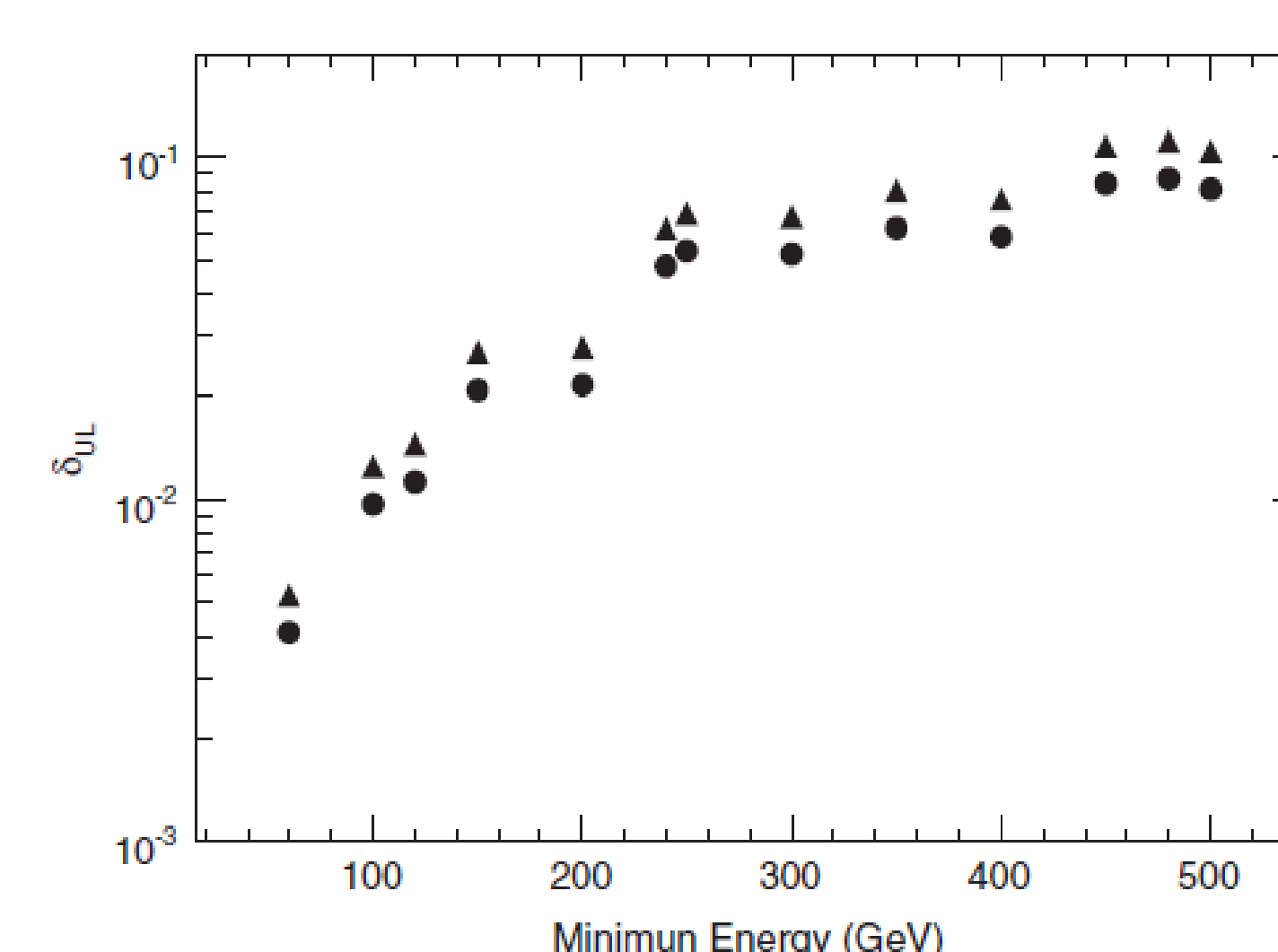


FIG. 4 Upper limits on the dipole anisotropy versus the minimum energy for different confidence levels; ● 90% CL; ▲ 95% CL.

3. Measurements with 29 months and behavior at low energy

Starting from second year of data taking (Sep. 2009) the Fermi telescope operates in survey mode with large rocking angle (angle between the Zenith direction and the LAT Z-axis) of 50° against 35° used during the first year: one orbit rocked by 35° (50°) towards the north orbital pole and the next rocked by 35° (50°) towards the south orbital pole. In this way the Earth is out the LAT field of view (FoV) as well. However, the large rocking angle value configuration allows to explore the region of large Zenith angles (and consequently low Nadir angles) because the large LAT FoV (the maximum observed off-axis angle, i.e. the angle with respect to the LAT Z-axis direction, is about 80°).

Let us assume an isotropic distribution of charged particles at very large distances from the Earth. Because of the action of the geomagnetic field, not all these particles are allowed to reach the Earth. At any point of the orbit, particles with given energy reaching that point must come from directions within a surface which forms the boundary between the region where all directions are allowed, and the region where only some or no direction are allowed. In case of CREs there is a pure region in the West where only positrons are allowed, as well as for electrons in the East. The sizes of these regions depend on the particle energy and LAT position. As the energy increases the size of the pure allowed region decreases.

To study the effect of the geomagnetic field on the arrival directions of the CREs, the observed count maps in the local Nadir-Azimuth coordinate system are compared with the “no-anisotropy” maps built with the shuffling method. The analyzed data set corresponds to the first 2.5 years of LAT science operation (survey mode) starting from August 2008. Figure 5 shows the significance maps for different energy bands produced by comparing the actual count maps with the “no-anisotropy” ones. The shape of the significance maps is due to the presence of regions where only electrons/positrons are allowed with regions where both particles are allowed, and to the fact that CREs are mainly composed of electrons. The significance decreases at low Nadir angles, because of the lack of statistics due to the Fermi rocking profile that keeps the Earth outside the FoV.

The positron regions are located in the Western hemisphere where large deficits are observed since their fraction is about few tens % with respect to the electrons. The deficit regions become more extended using limited data not taken in survey mode (i.e. Nadir pointing mode, Target of Opportunity, Automated Repointing Request), where low Nadir angles can be explored (see presentation by W. Mitthumsiri et al.). In this analysis the positron (deficit) regions are well observed up to energies of about 100 GeV due to the large rocking angle configuration, while in the small rocking angle configuration they were observed only at low energies (<60 GeV). These deficits are responsible of large anisotropies when looking in Galactic or Equatorial coordinates. Therefore additional cuts are needed when searching for CREs anisotropies, for instance reducing the FoV of the LAT to preserve uniform sky exposure across the field of view.

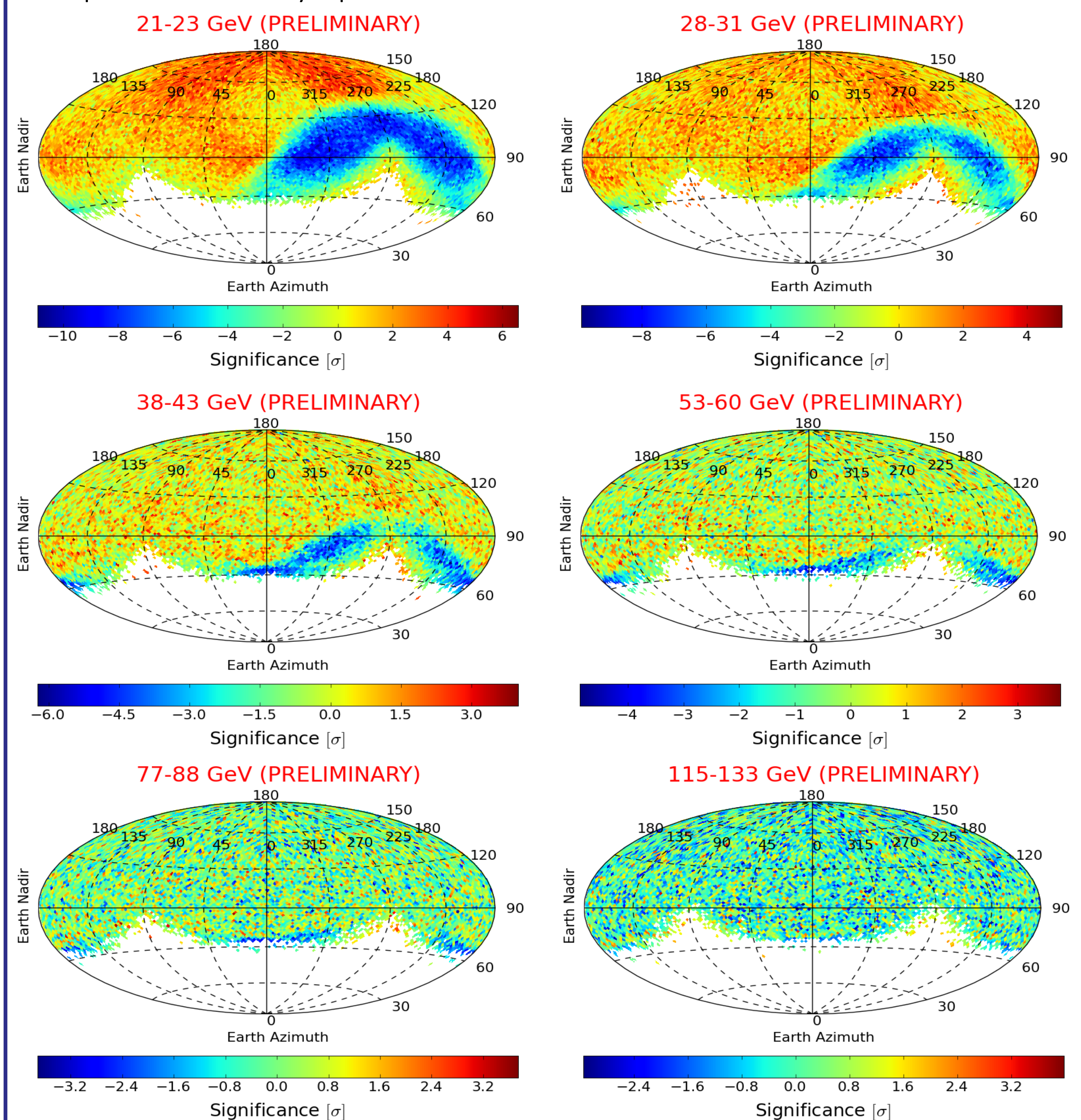


FIG. 5 Significance maps produced by comparing the actual count maps with the “no-anisotropy” count maps, for different energy bands (the energy increases from the top/left to the bottom/right). The maps consist of 12288 independent pixels with same area, according to the HEALPix pixelization scheme (K. M. Górski, E. Hivon, A. J. Banday, B. D. Wandelt, F. K. Hansen, M. Reinecke, and M. Bartelmann, *Astrophys. J.* 622, 759 (2005); <http://healpix.jpl.nasa.gov>) with $N_{\text{side}}=32$. The shape of the significance maps result from the combination of pure electron/positron regions with regions where both particles are allowed.